RSC Advances

PAPER

View Article Online
View Journal | View Issue

Cite this: *RSC Adv.*, 2021, **11**, 26403

Two-photon excitable boron complex based on tridentate imidazo[1,5-*a*]pyridine ligand for heavy-atom-free mitochondria-targeted photodynamic therapy†

Keita Hoshi,[a] Masami Itaya,[a] Koki Tahara,[a] Airi Matsumoto,[b] Atsuhi Tabata,[b] Hideaki Nagamune,[b] Yasushi Yoshida,[c] Eiji Hase,[d] Takeo Minamikawa,[d] Takeshi Yasui,[d] Tetsuro Katayama,*[d] Akihiro Furube,[d] Keiji Minagawa,[a] Yasushi Imada[a] and Fumitoshi Yagishita*[ad]

Received 30th June 2021
Accepted 22nd July 2021

DOI: 10.1039/d1ra05059a

rsc.li/rsc-advances

We have synthesized a cyan fluorescent boron complex based on a tridentate imidazo[1,5-*a*]pyridine ligand. The boron complex was found to have potential applications as not only a chiroptical material but also a heavy-atom-free mitochondria-targeted photosensitizer for cancer treatment.

Small organic molecules showing photoluminescence have drawn considerable attention due to their application in material science and bioscience. Among them, introduction of boron atoms into the π-conjugated system is recognized to improve the photophysical properties dramatically. Thus, numerous boron complexes including BODIPY dyes, which are one of the well-known fluorescent boron complexes based on the dipyrromethene ligand, have been designed and evaluated for their potential applications in organic light-emitting diodes (OLEDs),[1] solar cells,[2] medicinal diagnosis[3] and photodynamic therapy (PDT).[4] Various BODIPY analogues based on the dipyrromethene ligand have been developed to achieve the applications mentioned above, whereas the research on the development of novel luminescent boron complexes based on aromatic ligands has emerged to explore and improve the photofunctionalities. For example, some successful examples of rigid four-coordinated boron complexes based on tridentate ligands, which show unique and useful luminescent properties such as self-assembly,[5] aggregation-induced emission[6] and chiroptical properties,[7] have been reported.

PDT has a huge importance in the healthcare field due to its noninvasive treatment for various diseases including cancer.[8] In the PDT process the photosensitizers play a key role to generate the reactive oxygen species (ROS) *via* energy transfer from the triplet photosensitizer to molecular oxygen. Although the introduction of heavy halogen atoms into the dye is one of the promising strategies to enhance intersystem crossing for improving the singlet oxygen generation capability, this method often causes dark toxicity. Thus, the research on the development of the heavy-atom-free photosensitizers has become increasingly important. Recently, some heavy-atom-free triplet BODIPY dyes have been designed and synthesized based on the molecular concept such as the photo-induced electron transfer (PET) process, reducing the energy gap between the lowest singlet excited state and the lowest triplet excited state, and replacement of the oxygen atom of the carbonyl group with a sulfur atom to enhance the intersystem crossing.[9] However, the designing of heavy-atom-free photosensitizers is still a challenging research area.

In this manuscript, we describe the synthesis, crystal structure and photophysical properties of the luminescent boron

[a]*Department of Applied Chemistry, Tokushima University, 2-1 Minamijosanjima, Tokushima 770-8506, Japan. E-mail: yagishitaf@tokushima-u.ac.jp*

[b]*Department of Bioscience and Bioindustry, Tokushima University, 2-1 Minamijosanjima, Tokushima 770-8513, Japan*

[c]*Department of Applied Chemistry and Biotechnology, Graduate School of Engineering, Chiba University, 1-33 Yayoi-cho, Inage-ku, Chiba 263-8522, Japan*

[d]*Department of Post-LED Photonics Research, Institute of Post-LED Photonics, Tokushima University, 2-1 Minamijosanjima, Tokushima 770-8506, Japan*

† Electronic supplementary information (ESI) available: Additional figures, crystallographic data in CIF, and NMR spectra. CCDC 2085924. For ESI and crystallographic data in CIF or other electronic format see DOI: 10.1039/d1ra05059a

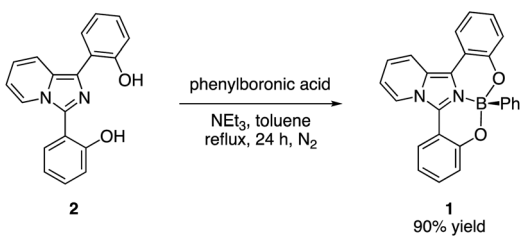

2 → 1 (90% yield)

Scheme 1 Synthesis of the boron complex **1**.

complex **1** based on 1,3-bis(*o*-hydroxyphenyl)imidazo[1,5-*a*]pyridine ligand **2**, which works as a tridentate *O*,*N*,*O*-ligand (Scheme 1). In addition, it was found that the boron complex **1** not only shows a cyan emission from the singlet excited state but also forms a triplet excited state *via* intersystem crossing, which is applicable in biological application as a heavy-atom-free photosensitizer for a potent cancer treatment.

The tridentate ligand **2** was synthesized from commercially available imidazo[1,5-*a*]pyridine *via* three steps including the iodination reaction, Suzuki–Miyaura cross coupling reaction using the *o*-methoxyphenylboronic acid and demethylation reaction using boron tribromide (Scheme S1†). As shown in Scheme 1, the desired boron complex **1** was prepared by the reaction of tridentate ligand **2** with phenylboronic acid in 90% yield. The structure of **1** was determined by NMR spectroscopy and HRMS. Fortunately, the single crystals of **1** suitable for the X-ray crystallographic analysis were prepared from dichloromethane and hexane. The X-ray analysis of **1** revealed that the boron atom is bound to the sp^2 nitrogen atom of the imidazo[1,5-*a*]pyridine ring and two oxygen atoms of the *o*-hydroxyphenyl groups to form a tetracoordinate boron complex (Fig. 1). The N–B bond length is 1.547 Å and slightly longer than that of the O–B bond (1.475 Å for O1–B bond and 1.463 Å for O2–B bond, respectively). The dihedral angles between the imidazo[1,5-*a*]pyridine core and each substituted phenyl ring at 1- and 3-positions are 10.27° for N–C1–C2–C3 and 14.59° for N–C4–C5–C6. It should be noted that the rigid perpendicular orientation of the axial phenyl ring at boron atom to the unsymmetrical imidazo[1,5-*a*]pyridine ligand leads to chiral scaffold. Indeed, the pair of the positive and negative CD peaks at 254 nm, which indicate the opposite of optical rotation derived from both enantiomers of **1**, were observed by HPLC using a chiral stationary phase (Daicel Corp. CHIRALPAK IB) (Fig. S1†). We also conducted the optical resolution of **1** and the ECD spectra were shown in Fig S2.† The experimental ECD spectra were similar to the calculated ECD spectra shown in Fig. S8.† The calculated ECD spectra indicated that the (*R*)-**1** and (*S*)-**1** show the positive and negative ECD signals at around 370 nm, respectively. Thus, we speculate that the first and second fractions observed in HPLC analysis correspond to (*R*)-**1** and (*S*)-**1**, respectively. Although we did not conduct the CPL measurement of the boron complex **1**, these findings indicate the potential application of **1** as a new class of luminescent boron complex showing a chiroptical property.

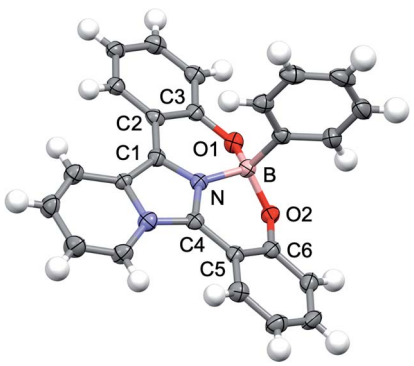

Fig. 1 ORTEP drawing of **1**. Disordered dichloromethane molecule is omitted for clarity.

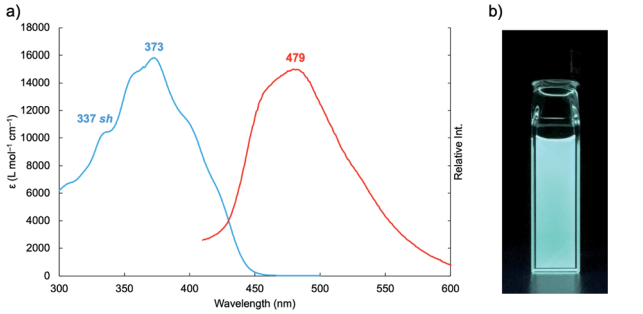

Fig. 2 (a) Absorption (blue line) and PL (red line) spectra of **1** in DMSO "sh" denotes a shoulder band. (b) Photoluminescence of **1** in DMSO under 365 nm irradiation.

Next, we investigated the photophysical property of **1**. The photophysical data of **1** in dimethyl sulfoxide (DMSO) are summarized in Table S1† accompanied by its absorption and photoluminescence (PL) spectra in Fig. 2. The absorption maximum of **1** was observed at 373 nm with moderate molar extinction coefficient (ε_{max} = 15 800 L mol^{-1} cm^{-1}) concomitantly with some shoulder bands. The boron complex **1** exhibits cyan emission, and PL peak was observed at 479 nm. Although we also examined the solvent effect using some organic solvents, obvious solvent polarity-dependent absorption and PL emission of **1** were not observed (Fig. S3†). The absolute PL quantum yield is found to be 0.34 in DMSO. The fluorescent lifetime of **1** (τ_f = 5.01 ns) is shorter than those of boron complexes of 1-(*o*-hydroxyphenyl)imidazo[1,5-*a*]pyridine (τ_f = 10.1–12.5 ns),[10] the value is within a range of the fluorescence lifetimes of known BODIPY dyes (around 1–10 ns).[11] The boron complex of 1-(*o*-hydroxyphenyl)imidazo[1,5-*a*]pyridine shows high fluorescence quantum yields (Φ_{em} = up to 0.71),[10] whereas the boron complex **1** shows medium fluorescence quantum yield in solution (Φ_{em} = 0.34). The decrease of PL quantum yield suggests the increase in non-radiative rate constant. Although the absolute PL value is decreased in solid state (Φ_{em} = 0.05), the boron complex **1** shows cyan emission even in the solid state. Decreasing of the PL quantum yield in the solid state suggests that the structural relaxation process of imidazo[1,5-*a*]pyridine unit is important for the radiative process. Such a non-radiative process is considered as intramolecular vibrational redistribution (IVR) or intersystem crossing process. Thus, we measured femtosecond transient absorption spectra of **1** in DMSO to elucidate the non-radiative process on the excited state. The setup for the measurement of transient absorption spectra is shown in Fig. S4,† and the time-resolved transient spectra of **1** in DMSO are shown in Fig. 3a. The absorption band appeared immediately around 690 nm after excitation. Decay components with a time constant of 480 ps was obtained with exponential fitting as shown in Fig. 3b. Sub nanoseconds relaxation process is slower than general IVR and suggests the change of intramolecular charge transfer (CT) character.[12]

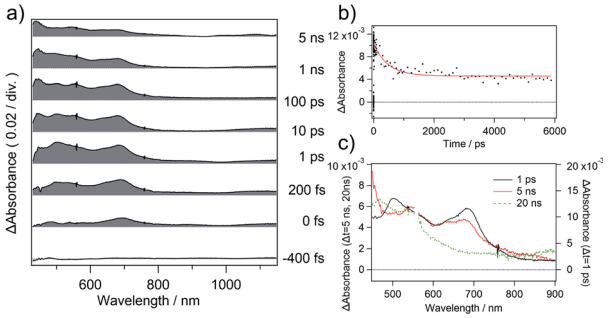

Fig. 3 (a) and (c) Femtosecond transient absorption spectra of **1** in DMSO after excitation at 400 nm. (b) Transient absorption decay profile (scattered points) at 693 nm and fit (solid line) with an exponential function with a time constant 480 ps.

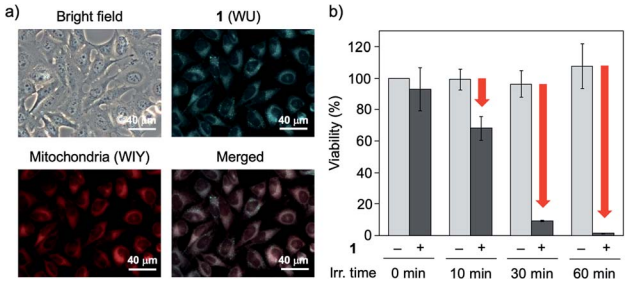

Fig. 4 (a) Observed images focused on mitochondria in HeLa cells with **1** and a mitochondrial marker. Cyan fluorescence of **1** was observed through a WU filter and red florescence of a mitochondrial marker was observed through a WIY filter. (b) Cell viabilities of HeLa cells after UVA-LED irradiation with (+) or without (−) staining by **1**.

Then, the absorption band at 545 nm arose in place of the decrease in band around 690 nm according to an increase in the delay time after excitation. Because the transient absorption band at 545 nm survives substantially longer than the fluorescence lifetime, the transient absorption spectrum observed at a time delay of 20 ns is ascribed to the triplet excited state of **1** (Fig. 3c). Intersystem crossing process might be induced with the increase of intramolecular charge transfer character.[13] The yield of intersystem crossing is roughly estimated to be up to 0.36 from PL yield and deactivation process in transient absorbance at 693 nm. This finding encouraged us to elucidate the potential application of **1** as a heavy-atom-free photosensitizer for PDT treatment through triplet state.

To perform the biological application, the dark toxicity is undesirable nature. Thus, we evaluated the cytotoxicity of **1** to HeLa cells using CCK-8 assay. The viabilities of HeLa cells incubated for 1 hour (for acute toxicity) and 24 hours (for subacute toxicity) with various concentrations of **1** are summarized in Fig. S5.† As a result, the boron complex **1** did not show the significant toxicity to HeLa cells in each concentration tested in this study under a dark. We next applied the boron complex **1** to a fluorescence bioimaging experiment of HeLa cells because the cellular localization of photosensitizer is important to achieve the effective PDT treatment. Among the organelle, mitochondria, which plays a key role in activating apoptosis, has been recognized as a promising target for the designing PDT agents.[14] When HeLa cells were incubated with **1** (5.0×10^{-5} mol L^{-1}) at 37 °C for 1 hour under 5% CO_2 conditions, the cells were labelled with cyan fluorescence signals indicating **1**. To elucidate the cellular localization of **1**, we conducted the co-staining experiment of HeLa cells using **1** and a mitochondrial marker (MitoTracker Red, ThermoFisher Scientific). When HeLa cells were incubated with boron complex **1** and the mitochondrial marker at 37 °C for 1 hour under 5% CO_2 conditions, it was found that the cyan fluorescence signals indicating **1** co-localized with the red fluorescence signals indicating the mitochondrial marker (Fig. 4a). It is reported that the neutral BODIPY dye tends to localize into the mitochondria of cells to its low electron density nature.[15] Because the TD-DFT calculation indicates the ICT nature of **1** in the excited state, which may be caused by partial electron deficiency of fluorophore, we consider that the boron complex **1** also shows high affinity toward mitochondria (Fig. S6†). In addition, this finding indicates the potential application of **1** as a heavy-atom-free mitochondria-targeted PDT agent against cancer cells.

We next focused on the application of **1** as a one-photon PDT agent using UVA-LED. The photocytotoxicity against HeLa cells was not observed in the absence of **1** after the UVA-LED irradiation for 60 minutes (Fig. 4b). Conversely, the cell viabilities of HeLa cells stained by **1** were gradually decreased according to the continuous UVA-LED irradiation, and the significant cytotoxicity of **1** was observed after UVA-LED irradiation for 60 minutes (Fig. 4b). To validate a role of **1** as mitochondria-targeted PDT agent, we also conducted the JC-1 assay for the measurement of the mitochondrial membrane potential to evaluate the mitochondrial function after the continuous UVA-LED irradiation. When the UVA-LED irradiation on HeLa cells in the absence of **1** was conducted for 0, 10 and 30 minutes, the changes of red and green fluorescence signals of JC-1 dyes were not observed (Fig. 5a). On the other hand, the continuous UVA-LED irradiation on HeLa cells stained by **1** (5.0×10^{-5} mol L^{-1}) elevated the depolarization of the mitochondrial membrane potential (Fig. 5b). Mitochondrial damages of HeLa cells were similarly observed even in the presence of lower concentrations of **1** (5.0×10^{-6} mol L^{-1}) after 30 min irradiation (Fig. S10†).

The use of UVA light source was unfavorable for PDT treatment due to its low light penetration and potential toxicity. On

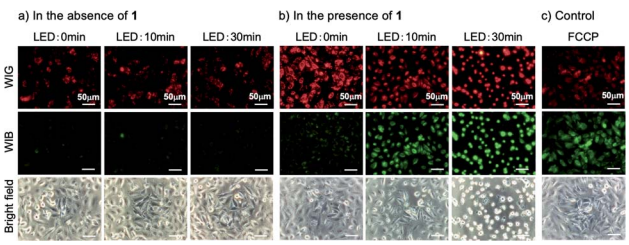

Fig. 5 Photographs of HeLa cells incubated with the JC-1 dye (a) in the absence and (b) presence of **1**; fluorescence images through WIG filter (upper), those through WIB filter (middle) and bright fields (lower).

the other hand, it is known that the two-photon excitation process enables the excitation of dye at lower energy.[16] The two-photon technology realizes the PDT treatment with some beneficial outcomes such as high penetration depth, spatial selectivity, and low phototoxicity to healthy tissues.[17] Thus, we investigated the two-photon excitable nature to evaluate the potential of **1** as two-photon PDT agent for cancer treatment. The two-photon excitation of **1** was studied using a femtosecond pulse laser source, and the setup is shown in Fig. S11.† When the DMSO solution of **1** was excited at 740 nm, cyan fluorescence was observed at the focal point of the laser. The log–log plot of the fluorescence intensity against the laser power gave a linear line with a slope of 1.92, which indicates the occurrence to two-photon absorption of **1** (Fig. S12†). When we conducted the two-photon imaging of mitochondria in HeLa cells, fluorescence image was successfully observed under 740 nm irradiation condition (Fig. S13†). These results strongly indicated the potential application of **1** as multi-photon excitable photosensitizer, *i.e.*, NIR excitable PDT agent for cancer treatment.

In conclusion, we have synthesized and characterized the boron complex based on the tridentate imidazo[1,5-*a*]pyridine ligand. X-ray analysis of **1** revealed that the perpendicular orientation of the axial phenyl ring at boron atom to the unsymmetrical planar ligand constructs a chiral environment. The boron complex **1** was found to work as the heavy-atom-free photosensitizer based on the experimental study of its excited state dynamics. The boron complex **1** showed not only a photocytotoxicity through triplet state but also a two-photon absorption nature. In addition, the PDT agents exhibiting photoluminescence have the advantages because they can visualize and define the affected area during the PDT treatment, and have potential application in theranostics, which combines the therapeutic and diagnostic imaging medical techniques.[18] Thus, we believe that the boron complex **1** becomes the new molecular design for a theranostics agent.

Author contributions

F. Y. and T. K. conceived the project, performed all experiments, and wrote the manuscript. K. H., M. I., H. T. and Y. Y. carried out the synthesis and characterization of the compounds. A. M., A. T. and H. N. carried out the bioassay. E. H., T. M. and T. Y. carried out the two-photon excitation experiments. A. F measured the transient absorption spectra. K. M. and Y. I. supervised the experiments. All authors read and approved the final manuscript.

Conflicts of interest

There are no conflicts to declare.

Acknowledgements

The authors would like to thank Dr H. Sato (Rigaku Corp.) for supporting the X-ray analysis, the NICHIA corp. for supplying LEDs, Prof. M. Ogasawara (Tokushima Univ.) for the optical resolution of 1, and a research grant from the Research Clusters Program of Tokushima University (No. 1802001, 1802003, and 2003006). This work was supported by the project on the Promotion of Regional Industries and Universities from the Cabinet Office, Japan, by the Creation and Application of Next-Generation Photonics by Tokushima Prefecture from the Tokushima Prefectural Government, Japan, and by JSPS KAKENHI, Grant Numbers 19K20691 and 20H02767.

Notes and references

1 (*a*) C.-L. Liu, Y. Chen, D. P. Shelar, C. Li, G. Cheng and W.-F. Fu, *J. Mater. Chem. C*, 2014, **2**, 5471; (*b*) M. Chapran, E. Angioni, N. J. Findlay, B. Breig, V. Cherpak, P. Stakhira, T. Tuttle, D. Volyniuk, J. V. Grazulevicius, Y. A. Nastishin, O. D. Lavrentovich and P. J. Skabara, *ACS Appl. Mater. Interfaces*, 2017, **9**, 4750; (*c*) D.-H. Kim, A. D'Aléo, X.-K. Chen, A. D. S. Sandanayaka, D. Yao, L. Zhao, T. Komino, E. Zaborova, G. Canard, Y. Tsuchiya, E. Choi, J. W. Wu, F. Fages, J.-L. Brédas, J.-C. Ribierre and C. Adachi, *Nat. Photonics*, 2018, **12**, 98.

2 (*a*) S. Erten-Ela, M. D. Yilmaz, B. Icli, Y. Dede, S. Icli and E. U. Akkaya, *Org. Lett.*, 2008, **10**, 3299; (*b*) S. Kolemen, O. A. Bozdemir, Y. Cakmak, G. Barin, S. Erten-Ela, M. Marszalek, J.-H. Yum, S. M. Zakeeruddin, M. K. Nazeeruddin, M. Grätzel and E. U. Akkaya, *Chem. Sci.*, 2011, **2**, 949; (*c*) I. Bulut, Q. Huaulmé, A. Mirloup, P. Chávez, S. Fall, A. Hébraud, S. Méry, B. Heinrich, T. Heiser, P. Lévêque and N. Leclerc, *ChemSusChem*, 2017, **10**, 1878.

3 T. Kowada, H. Maeda and K. Kikuchi, *Chem. Soc. Rev.*, 2015, **44**, 4953.

4 A. Kamkaew, S. H. Lim, H. B. Lee, L. V. Kiew, L. Y. Chung and K. Burgess, *Chem. Soc. Rev.*, 2013, **42**, 77.

5 C. Glotzbach, U. Kauscher, J. Voskuhl, N. S. Kehr, M. C. A. Stuart, R. Fröhlich, H. J. Galla, B. J. Ravoo, K. Nagura, S. Saito, S. Yamaguchi and E.-U. Würthwein, *J. Org. Chem.*, 2013, **78**, 4410.

6 (*a*) M. Gon, K. Tanaka and Y. Chujo, *Angew. Chem., Int. Ed.*, 2018, **57**, 6546; (*b*) S. Ohtani, M. Gon, K. Tanaka and Y. Chujo, *Crystals*, 2020, **10**, 615.

7 (*a*) R. Clarke, K. L. Ho, A. A. Alsimaree, O. J. Woodford, P. G. Waddell, J. Bogaerts, W. Herrebout, J. G. Knight, R. Pal, T. J. Penfold and M. J. Hall, *ChemPhotoChem*, 2017, **1**, 513; (*b*) Y. Gobo, R. Matsuoka, Y. Chiba, T. Nakamura and T. Nabeshima, *Tetrahedron Lett.*, 2018, **59**, 4149; (*c*) V. G. Jiménez, F. M. F. Santos, S. Castro-Fernández, J. M. Cuerva, P. M. P. Gois, U. Pischel and A. G. Campaña, *J. Org. Chem.*, 2018, **83**, 14057; (*d*) S. Ohtani, Y. Takeda, M. Gon, K. Tanaka and Y. Chujo, *Chem. Commun.*, 2020, **56**, 15305; (*e*) N. Algoazy, J. G. Knight, P. G. Waddell, R. Aerts, W. Herrebout, H. H. T. Al-Sharif, J. K. G. Karlsson and A. Harriman, *Chem.–Eur. J.*, 2021, **27**, 5246.

8 D. E. J. G. J. Dolmans, D. Fukumura and R. K. Jain, *Nat. Rev. Cancer*, 2003, **3**, 380.

9 (*a*) M. A. Filatov, *Org. Biomol. Chem.*, 2020, **18**, 10; (*b*) V.-N. Nguyen, Y. Yan, J. Zhao and J. Yoon, *Acc. Chem. Res.*, 2021, **54**, 207.

10 F. Yagishita, T. Kinouchi, K. Hoshi, Y. Tezuka, Y. Jibu, T. Karatsu, N. Uemura, Y. Yoshida, T. Mino, M. Sakamoto and Y. Kawamura, *Tetrahedron*, 2018, **74**, 3728.
11 G. Ulrichi, R. Ziessel and A. Harriman, *Angew. Chem., Int. Ed.*, 2008, **47**, 1184.
12 T. Kushida, C. Camacho, A. Shuto, S. Irle, M. Muramatsu, T. Katayama, S. Ito, Y. Nagasawa, H. Miyasaka, E. Sakuda, N. Kitamura, Z. Zhou, A. Wakamiya and S. Yamaguchi, *Chem. Sci.*, 2014, **5**, 1296.
13 Z. Wang, M. Ivanov, Y. Gao, L. Bussotti, P. Foggi, H. Zhang, N. Russo, B. Dick, J. Zhao, M. Di Donato, G. Mazzone, L. Luo and M. Fedin, *Chem.–Eur. J.*, 2020, **26**, 1091.
14 (*a*) W. Lv, Z. Zhang, K. Y. Zhang, H. Yang, S. Liu, A. Xu, S. Guo, Q. Zhao and W. Huang, *Angew. Chem., Int. Ed.*, 2016, **55**, 9947; (*b*) W. Zhuang, L. Yang, B. Ma, Q. Kong, G. Li, Y. Wang and B. Z. Tang, *ACS Appl. Mater. Interfaces*, 2019, **11**, 20715; (*c*) S. Qi, N. Kwon, Y. Yim, V.-N. Nguyen and J. Yoon, *Chem. Sci.*, 2020, **11**, 6479.
15 T. Gayathri, S. Karnewar, S. Kotamraju and S. P. Singh, *ACS Med. Chem. Lett.*, 2018, **9**, 618.
16 W. Denk, J. H. Strickler and W. W. Webb, *Science*, 1990, **248**, 73.
17 F. Bolze, S. Jenni, A. Sour and V. Heitz, *Chem. Commun.*, 2017, **53**, 12857.
18 J. Zhang, L. Ning, J. Huang, C. Zhang and K. Pu, *Chem. Sci.*, 2020, **11**, 618.